Journal of Peptide Science
J. Peptide Sci. **9**: 90–105 (2003)
Published online in Wiley InterScience (www.interscience.wiley.com). DOI: 10.1002/psc.434

JOURNAL OF PEPTIDE SCIENCE

Synthetic Peptides Mimicking the Interleukin-6/gp130 Interaction: a Two-Helix Bundle System. Design and Conformational Studies

LAURA ZACCARO,[a†] ENRICO BUCCI,[a†] ROSA MARIA VITALE,[b] GIUSEPPE PERRETTA,[a] ROBERTO FATTORUSSO,[b] ETTORE BENEDETTI,[a] MICHELE SAVIANO[a]* and CARLO PEDONE[a]

[a] Istituto di Biostrutture e Bioimmagini, C.N.R., and Dipartimento di Chimica Biologica, Università ``Federico II'' di Napoli, 80134 Napoli, Italy
[b] Dipartimento di Scienze Ambientali, Seconda Università di Napoli, 81100 Caserta, Italy

Received 17 June 2002
Accepted 29 June 2002

Abstract: The objective of our study was to mimic in a typical reductionist approach the molecular interactions observed at the interface between the gp130 receptor and interleukin-6 during formation of their complex. A peptide system obtained by reproducing some of the interleukin-6/gp130 molecular interactions into a two-helix bundle structure was investigated. The solution conformational features of this system were determined by CD and NMR techniques. The CD titration experiments demonstrated that the interaction between the designed peptides is specific and based on a well-defined stoichiometry. The NMR data confirmed some of the structural features of the binding mechanism as predicted by the rational design and indicated that under our conditions the recognition specificity and affinity can be explained by the formation of a two-helix bundle. Thus, the data reported herein represent a promising indication on how to develop new peptides able to interfere with formation of the interleukin-6/gp130 complex. Copyright © 2003 European Peptide Society and John Wiley & Sons, Ltd.

Keywords: circular dichroism; cytokine; gp130; interleukin-6; molecular design; nuclear magnetic resonance; two-helix bundle

Abbreviations: Aib, α-aminoisobutyric acid or $C^{\alpha,\alpha}$ -dimethylglycine; Boc, *tert*-butyloxycarbonyl; CD, circular dichroism; CVFF, consistent valence force field; DG, distance geometry; DIEA, *N*,*N*-diisopropylethylamine; DMF, *N*,*N*-dimethylformamide; DQF-COSY, double-quantum filtered correlated spectroscopy; EDT, 1,2-ethanedithiol; FID, free induction decay; HATU, 2-(1H-9-azabenzotriazol-1-yl)-1,1,3,3-tetramethyluronium; hIL6, human interleukin-6; HMQC, heteronuclear multiple-quantum correlated; HOBt, 1-hydroxybenzotriazole; IL6, interleukin-6; MALDI-Tof, matrix-assisted laser desorption ionization time-of-flight; MBHA, 4-methylbenzhydrylamine; NOESY, nuclear Overhauser enhancement spectroscopy; O*t*Bu, *tert*-butoxy; PAL, 5-(4-aminomethyl-3,5-dimethoxyphenoxy)valeryl; PEG, polyethylene glycol; Pmc, 2,2,5,7,8-pentamethylchroman-6-sulfonyl; PS, polystyrene; PyBop, benzotriazol-1-yl-oxy-tris-pyrrolidino-phosphonium; RMSD, root mean square deviation; ROESY, rotating frame nuclear Overhauser enhancement spectroscopy; RP-HPLC, reverse phase high-pressure liquid chromatography; TFA, trifluoroacetic acid; TFE, 2,2,2-trifluoroethanol; TMS, tetramethylsilane; TOCSY, total correlation spectroscopy; Trt, trityl or triphenylmethyl; Z, benzyloxycarbonyl. Amino acids are in the L configuration.

* Correspondence to: Dr. Michele Saviano, Istituto di Biostrutture e Bioimmagini, CNR, via Mezzocannone 6, 80134 Napoli, Italy; e-mail: saviano@chemistry.unina.it

† These two authors contributed equally to this work.

Contract/grant sponsor: MURST; Contract/grant number: PRIN 2000.
Contract/grant sponsor: CNR Italy.
Contract/grant sponsor: Regione Campania Legge; Contract/grant number: 41/94.
Contract/grant sponsor: Programma Biotecnologie Legge; Contract/grant number: 95/95.

Copyright © 2003 European Peptide Society and John Wiley & Sons, Ltd.

INTRODUCTION

Success in drug design is frequently related to reproducing and/or modulating interactions between different macromolecules.

In this frame it is particularly relevant to assess the level of our ability to mimic the binding properties of one or more partners of biological complexes in a small synthetic system. Interleukin-6 (IL6) is a multifunctional protein which is involved in host infection defence, tissue damage and in a number of pathological processes [1,2]. It is a 26 Kd cytokine secreted by fibroblasts, monocytes, B-cells, endothelial cells, T-cells, microglia and astrocytes. IL6 is the principal cytokine inducing activated B-lymphocyte differentiation into cells able to produce antibodies. Moreover, it acts as a stimulating and growth-inducing factor for plasmocytoma and hybridoma and stimulates the factor-dependent myeloid cells [3,4]. Finally, IL6 promotes *in vivo* haematopoiesis and osteogenesis and is involved in the bone disruption process in the post-menopause osteoporosis [5,6].

The molecular recognition of IL6, and thus the various effects of cytokines on the cell, is mediated by a mechanism which is quite well understood: the formation of a high affinity complex between the IL6/IL6 receptor α (IL6Rα) low affinity heterodimer and the β receptor (gp130) is required for the multimerization complex *via* gp130 homodimerization [7–9]. The multimeric complex binds strongly to IL6 and efficiently triggers the signal to activate the intracytoplasmatic signal mediators [9].

Interleukin-6 and, more recently, the gp130 cytokine binding domain x-ray diffraction structures have been determined [10,11]. IL6 consists mainly of a four α-helix bundle (helix A–D). The IL6 contact surface with the receptor is formed by part of the solvent-exposed surface of specific helical components; in particular, there is experimental evidence that helix C is involved in the binding to the gp130 receptor [12–14]. In addition, solution conformational studies of peptide segments from the *N*- and *C*- termini of IL6 have shown that small parts of the protein may assume an ordered structure and retain biological activity [15,16]. These data suggest that a possible approach to the reduction of the IL6-binding surface is to model a helical peptide as far as possible related to helix C.

In the absence of detailed crystallographic information on the IL6 multimeric complex, all the available structural and biological data were used to carry out a three-dimensional molecular modelling study and computational simulations on hIL6, hIL6/hIL6Rα, hIL6/hIL6Rα/hgp130 and higher complexes [17]. The resulting homology models allowed the identification and quantitative analysis of the molecular determinants for the structure stabilization and ligand-receptor recognition [17].

Using these models, peptides were designed reproducing some of the observed IL6/gp130 interactions into a two-helix bundle structure by a 'minimalist approach'. To characterize the two-helix bundle complex, its conformational behaviour and three-dimensional structure are reported, as determined by CD analysis and homonuclear NMR spectroscopy. To the best of our knowledge, this represents the first example of structural characterization of a two-helix bundle system formed without the use of a rigid template or other linkers to connect to the *N*- and *C*-termini of the helices.

MATERIALS AND METHODS

Design

Energy minimizations were carried out with the program DISCOVER, version 2.98, implemented in the BIOSYM software package. Calculations were performed using CVFF [18–20] without cross- or Morse terms on a Silicon Graphics O2 workstation. The program INSIGHT II, version 98, was employed for model-building procedures and as a graphic interface. The minimization procedure consisted of a conjugate gradient minimization until the root-mean-square (rms) gradient of the potential energy was <0.001 kcal mol^{-1}.

Peptide Synthesis

The HAla and HIle peptide syntheses were performed on a Shimadzu PSSM8 automated solid-phase synthesizer; the HAib synthesis was carried out using a Milligen 9050 automated solid-phase synthesizer. Analytical RP-HPLC was performed on a Shimadzu LC instrument equipped with a diode array SPDM AV-10 and a SIL-10A autosampler. A Phenomenex C_{18} column (4.6$\times$ 250 mm; 5 µm; 300 Å) eluted with a H_2O/0.1% TFA (A) and CH_3CN/0.1% TFA (B) linear gradient, from 20% to 80% B over 20 min, at 1 ml min^{-1} flow rate, was used in the peptide analysis. Purification of the crude peptides was carried out on a Waters Delta Prep 4000 apparatus equipped with an UV Waters Mod 441 detector (Vydac C_{18} column 220 $\times$ 150 mm, 15 µm, 300 Å)

Copyright © 2003 European Peptide Society and John Wiley & Sons, Ltd.

using a 20 ml min^{-1} flow rate and the linear gradient mentioned above. MALDI-Tof spectra were obtained with a Perseptive spectrometer. All amino acids, Rink-amide MBHA resin, PyBop, HOBt were purchased from NovaBiochem; DIEA and TFA were Applied BioSystems products. Piperidine, pyridine and scavengers were from Fluka, while HATU and Fmoc-PAL-PEG-PS resin were from Primm. The solvents used in the synthesis, purification and characterization of the peptides were anhydrous and HPLC grade and were supplied by LabScan Analytica.

The peptides HIle [Ac-^{1}EEQARAK(Z)EMSTKVLIQ-FLQK^{20}-NH_2], HAla (Ac-^{1}DDEFARLTRAVLEAVAKS-SAK^{21}-NH_2) and HAib (Ac-^{1}DLRSUKEFUIRSLRASR-AMK^{20}-NH_2, where U is the Aib residue) were obtained with Fmoc-PAL-PEG-PS as the starting resin (substitution 0.195 mmol g^{-1}). Glass beads were added to the resin in a 1 : 1 (w/w) ratio with the initial dry solid support in order to improve the swelling properties. The side-chain protecting groups used were: Glu (OtBu), Arg (Pmc), Lys (Z), Lys (Boc), Gln (Trt), Thr (tBu), Ser (Trt) and Asp (OtBu). The syntheses were carried out with a fourfold excess of amino acid at every cycle and each residue was recirculated through the resin for 1 h twice. Cleavage of the peptides from the resin was accomplished by treating peptidyl resin for 3 h in a mixture of TFA and scavengers (TFA, water, EDT and triisopropylsilane 93 : 2.5 : 2.5 : 2 v/v).

The peptidyl resins were filtered off and the crude peptides were precipitated with diethyl ether, dissolved in a water/acetonitrile mixture and lyophilized. HPLC analysis showed a main peak at $R_t = 15.6$ min and a lower peak at $R_t = 16.7$ min, the latter corresponding to the desired product, for HIle, and a main peak at $R_t = 16.9$ min and $R_t = 12.9$ min for HAla and HAib, respectively.

The peptides were purified by preparative RP-HPLC; the collected fractions containing the peptides were lyophilized. The purity and the identity of the peptides were confirmed by analytical RP-HPLC and MALDI-Tof spectrometry.

Circular Dichroism

The CD spectra were obtained at 20 °C on a Jasco model J-700 spectropolarimeter equipped with a magnetic stirrer and a Neslab Rt111 temperature controller. The data were collected at 0.2 nm intervals, with a 10 nm min^{-1} scan rate, a 1 nm bandwidth and a 16 s response, from 260 to 190 nm using a 1 cm pathlength cuvette. The spectra were recorded in 5 mM sodium phosphate buffer at pH 6.7 with 20% TFE. CD intensities are expressed as mean residue ellipticities (deg × cm^2 × $dmol^{-1}$ of amino acid) calculated as molar ellipticity referring to the total amino acid concentration.

Stock solutions of the peptides were prepared in water. Then they were diluted in order to obtain a final solution with 80 : 20 phosphate buffer (5 mM)/TFE (v/v). CD solution concentrations were determined spectrophotometrically at 215 nm. Due to the overlapping absorbance contributions from the amide bond, the Phe side chain and the Z group, a calibration curve was required to obtain the molar extinction coefficients. The calculated molar extinctions were 36 032, 21 593 and 18 490 M^{-1} cm^{-1} for HIle, HAla and HAib, respectively. In the titration experiment increasing amounts (0.2 equivalents) of HAla (2.94×10^{-4} M) were added to a 3.16×10^{-6} M solution of HIle up to a 3 : 1 HAla/HIle ratio. The 1 : 1 mixture of HAla with the HAib unrelated peptide was prepared by adding to a solution of HAla (4.66×10^{-6} M) 1 equivalent of HAib peptide (5.97×10^{-4} M).

NMR

The peptide HIle was dissolved in a 5 mM sodium phosphate buffer (pH 6.64)-trifluoroethanol-d_3 (70 : 30, v/v) mixture (750 µl) at a concentration of 9.07×10^{-4} M as determined spectrophotometrically. No further increase of the helical content was detected by CD by adding more TFE. The peptide HAla was added to the HIle sample at a 1.1 : 1 concentration ratio.

The NMR experiments were recorded on a Varian Inova 600 spectrometer at a temperature of 298 K. Quadrature detection in the indirectly detected dimensions was carried out with States-TPPI hypercomplex phase incrementation [21]. Standard presaturation techniques were used for solvent suppression. TOCSY [22] and NOESY [23] spectra were acquired with a mixing time of 70 ms and of 250 ms, respectively. Double quantum filtered spectroscopy (DQF-COSY) [24] was acquired with 4096 data points in the direct dimension and 500 increments with 64 scans to obtain enough resolution to measure the $^{3}J_{HNH\alpha}$ coupling constants. All the spectra were processed with the software PROSA [25] and analysed with the program XEASY [26]. For the two dimensional experiments, the F2 dimension was zero-filled to 4096 real data points and the F1 dimension to 1024 real data points.

Copyright © 2003 European Peptide Society and John Wiley & Sons, Ltd.

Structure Calculations

249 NOE cross peak volumes were integrated with the program XEASY and processed by the DYANA [27] software calibrated on the volume of the terminal amide H_2-H_3 cross peak. The Lys(Z) residue was manually added to the DYANA residue library in order to account for the Z-group effect during the subsequent structure calculations. A total of 159 meaningful distance constraints and 64 angle constraints were obtained from the initial 249 NOE cross peaks and 20 coupling constants. These constraints were used to generate a total of 200 structures using the DYANA angle torsional dynamic procedure. The first 20 structures with the lowest target function values were refined by the energy minimization procedure of the SPDBV software. The minimization was carried out using the steepest descent algorithm (GROMOS96 force field) [28] until the energy difference between two subsequent steps was lower than 0.005 kJ/mol. The software MOLMOL [29] was used to produce the figures for the structures.

The package INSIGHT/DISCOVER (Accelrys Inc, USA) with CVFF [18–20] was used for energy minimization procedures to obtain a plausible model of the HIle/HAla complex. The minimization was carried out using the conjugate gradient method until the energy difference between two subsequent steps was lower than 0.01 kJ/mol.

A starting model for the computational studies was built using geometrical parameters for amino acid residues in the α-helix structure and using structural parameters from NMR data. The two peptides in α-helix were oriented using the INSIGHTII facility and graphics interface to satisfy the inter-helix NOE restraints and to avoid van der Waals overlap between the two molecules. The dihedral angles of the side chains were modelled by choosing favourable rotamers. A preliminary energy minimization was then carried out keeping all the backbone atoms fixed to refine the spatial position of the side chains. After this initial step full minimization was performed using NMR restraints.

RESULTS AND DISCUSSION

Peptide Design

Since there are no structural experimental data on the IL6/gp130 complex, as a starting point for the peptide design the theoretical model of the IL6 ternary complex (IL6/IL6Rα/gp130) proposed by Menziani *et al.* was used (Figure 1).

Attention was focused on IL6 helix C. As evident from the Menziani model and the biochemical data,

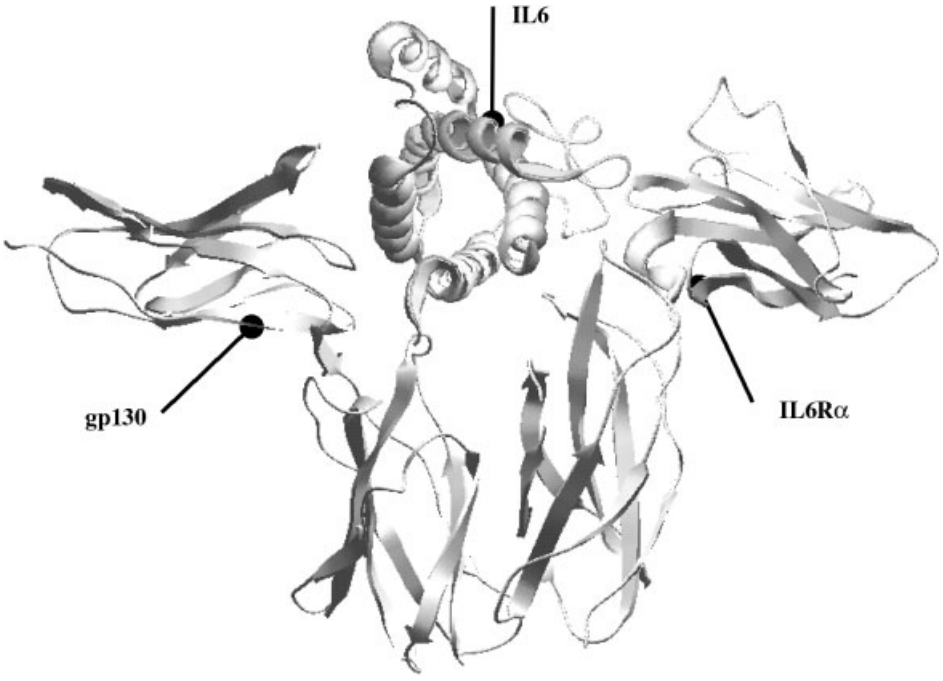

Figure 1 The theoretical trimeric molecular model of the Il6/Il6Rα/gp130 complex [17].

Copyright © 2003 European Peptide Society and John Wiley & Sons, Ltd.

helix C is involved in the interaction between IL6 and its receptor gp130, giving rise to the binding site 2 with helix A [12–14]. Helix C is an amphiphilic structure, with an extensive hydrophobic surface and a reduced hydrophilic surface (residues 91, 92, 95, 98, 102, 106, 110). The core of the hydrophobic surface (residues 94, 97, 101, 104 and 108) constitutes a strip of buried residues, used to pack the helix against the remaining protein.

The first peptide (HIle) was obtained by isolating helix C (91–110) from the IL6 x-ray diffraction structure. Then changes were introduced in the peptide sequence in order to modify the helical amphipathy. It has been demonstrated that the helical amphipathy of the peptides increases aggregation [30]. Helix C of IL6 has a highly amphipathic character and in solution may show self-aggregation. The peptide aggregation was decreased by replacing the Val^{97}residue, which in the whole protein is oriented towards the hydrophobic core, with a Lys residue protected with a bulky Z group. The helical stability of the isolated peptide was increased by replacing Gln^{98} with Glu to form an ionic pair (i, $i+4$) with Lys^{102} [31]. Finally, the peptide was *N*α-acetylated and *C*α-amidated to eliminate the terminal charges. The final HIle sequence was then Ac-^{1}EEQARAK(Z)EMSTKVLIQFLQK^{20}-NH_2.

Once a model was obtained for a peptide replacing the IL6 counterpart in the IL6/gp130 complex, modelling of a second peptide (HAla) potentially able to replace gp130 in the formation of the complex was carried out.

As a first step in the modelling procedure, by means of an energy interaction analysis at residue level those residues of the gp130 receptor in contact with helices A and C of IL6 were identified using the program CHARMM [32]. The selected sequences included the regions ^{61}VDYSTVYFVNIE^{72}, ^{41}WATHKFA^{47}, ^{16}GKKM^{19} and ^{91}FDPV^{94} (Figure 2) because of their close proximity to helix C. In particular, Ser^{64} and Tyr^{67} residues form H-bond interactions with Arg^{95} and Ser^{100} of IL6, respectively; the aromatic rings of Phe^{68} of the gp130 receptor and Phe^{107} of IL6 give rise to a π-stacking interaction. In addition, other selected regions having a number of residues involved into hydrophobic interactions are: gp130Val^{66}-IL6Val^{103}, gp130Phe^{46}-IL6Met^{99}, gp130Trp^{41}-IL6Val^{103}, gp130Val^{69}-IL6Phe^{107} and gp130Tyr^{62}-IL6Met^{99}.

As a second step, a 21-residue polyalanine sequence in the standard α-helix conformation was overlapped onto the surface defined by these regions using the most important IL6 contacting residues of gp130 as a reference for the overlapping procedure. The conformational analysis of these regions showed that the ϕ and ψ dihedral angles of the residues ^{64}STVYF^{68} and ^{16}GKK^{18} lie in the α-helical region of the Ramachandran map. As a consequence, all the backbone atoms and C$^{\beta}$

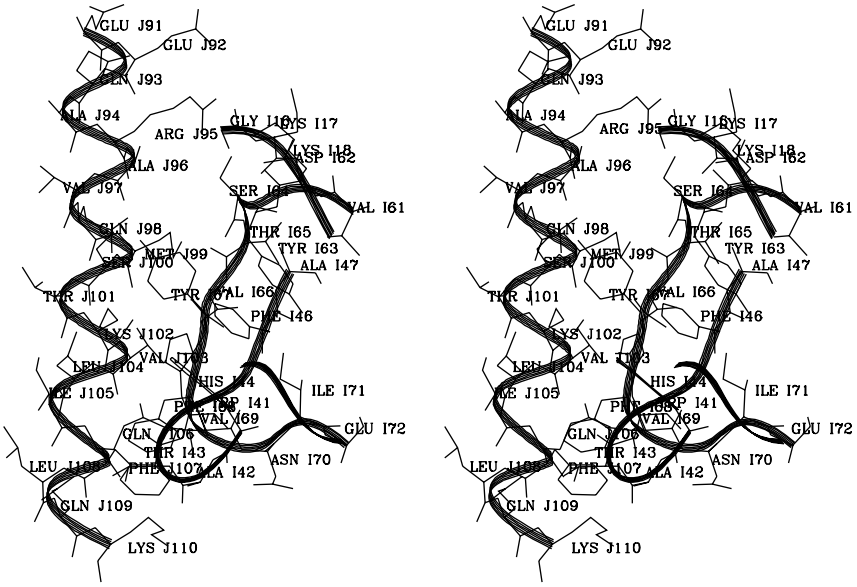

Figure 2 Stereo drawing of the selected regions of gp130 receptor close to IL6 helix C as obtained from the analysis of the model proposed by Menziani *et al.* [17].

Copyright © 2003 European Peptide Society and John Wiley & Sons, Ltd.

atoms of these selected residues were considered for the overlapping procedure. The polyalanine peptide orientation was set antiparallel with respect to helix C of IL6 because this is the favoured packing mode for α-helices in proteins [33]. The inter-helical crossing angle, a pseudo-dihedral angle between the axes of two helices, was very close to the value of 20° that is usually found in globular proteins.

As a third step, in the modelled helix the alanines in positions relevant for the interaction with IL6 were substituted with the corresponding residues of the gp130 receptor. In particular, the Ala residues in positions 3 and 9 of the helix were replaced with Phe and Val corresponding to Phe^{68} and Val^{66} of the gp130 receptor, respectively. In some selected cases we replaced the wild-type residues with others showing better features for the interaction: Ala^{6} corresponding to Val^{69} in the receptor sequence was mutated into a Leu to improve the hydrophobic interactions with Val^{103} and Phe^{107}; Ala^{8}, corresponding to Tyr^{67}, was replaced with a Thr residue to avoid steric repulsion in the packing between helices. The steric and electrostatic complementarities between HAla and HIle were improved by further replacements in the contact surface of HAla. In particular, two Ser residues were placed in positions 18 and 19 to form H-bond interactions with Arg^{5} and Glu^{2} residues of HIle, respectively. It is worth noting that all the substitutions with respect to the wild-type residues did not vary the hydrophobic nature of the residues were changed.

The final step of the modelling was aimed at reinforcing the helical propensity of the designed peptide. In particular, the side of the modelled peptide opposite to the interaction surface was modified by introducing the ionic pair $Glu^{12}\cdots Lys^{16}$ to increase the helical propensity [31]; the end-capping effect was obtained by flanking the helix termini with an Asp and a Lys at the *N*- and *C*-terminus, respectively [34]. To increase the helical content and the water solubility of the peptide without affecting the side interacting with HIle, the Ala residues at positions 1, 3, 6 and 9 were replaced with Asp, Glu, Arg and Arg, respectively. The Ala residue in position 12 was replaced with Leu to reduce the problems in the NMR assignment. Finally, HAla was *N*α-acetylated and *C*α-amidated to avoid additional charges not present in the reference structure. The final sequence of HAla was Ac-^{1}DDEFARLTRAVLEAVAKSSAK^{21}-NH_2. The resulting model of the HIle/HAla complex was minimized to refine its structure (Figure 3). The minimized model keeps all the desired interactions. In particular, in the model the axes of the two antiparallel α-helices form an angle of about 20°. The helix–helix complex is stabilized by several interactions: (i) H-bond interactions between Ser^{19} and Ser^{20} of HAla and

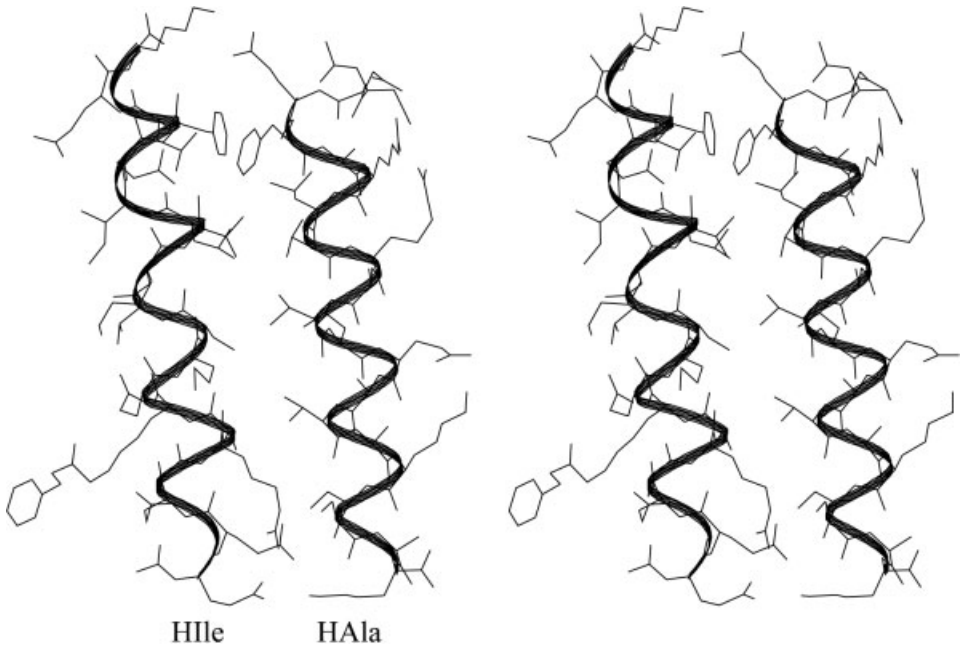

Figure 3 Stereo drawing of the molecular model of the two-helix bundle structure reproducing some of the observed IL6/gp130 interactions as obtained from the design procedure.

Copyright © 2003 European Peptide Society and John Wiley & Sons, Ltd.

Arg^5 and Glu^2 of HIle, respectively; (ii) hydrophobic interactions between residues of HAla (Leu^8, Phe^5, Val^{12} and Leu^8) and of HIle (Phe^{17}, Met^9 and Val^{13}). Other interactions between the two peptides are found in the *N*- and *C*- terminal regions. Indeed, additional H-bonds are present between the Glu^1 side chain in HIle and the Lys^{22} side chain in HAla, and between the Lys^{20} side chain in HIle and the Glu^2 side chain in HAla.

In addition, the two α-helices are stabilized by consecutive backbone C═O··· H-N intramolecular 5→1 H-bonds with the formation of α-turn structures [35]. The analysis of the ϕ, ψ dihedral angles of each residue in both peptide models shows that only the residues at the *N*- and *C*-termini present a deviation from the characteristic conformational angles for an α-helix ($\phi = -57^\circ$, $\psi = -47^\circ$). This distortion is partially due to the inter-helical H-bond interactions previously described.

Peptide Synthesis

The peptides were synthesized by means of the solid-phase method using Fmoc chemistry. Most of the Fmoc-protected amino acids were coupled according to the PyBop/HOBt/DIEA [36] method, but other residues (Gln^{18}, Arg^{16}, Leu^7, Ile^6, Gln^5, Gln^2, Lys^1 for HIle; Lys^{21}, Ala^{16}, Val^{15}, Ala^{14}, Leu^{12}, Ala^{10}, Glu^3, Asp^2 and Asp^1 for HAla; Arg^{11}, Aib^9, Phe^8, Aib^5, Arg^3, for HAib) were activated by the HATU/DIEA [37] method due to the intrinsic difficulties of the corresponding coupling steps.

A final Nα-acetylation step and purification by reversed-phase HPLC were performed for both peptides. After purification the yield of the HAla peptide was 52%, the yield of the HAib peptide was 65%, while that of the HIle peptide was 34% due to the formation of an unidentified deletion by-product. MALDI-Tof spectrometry showed molecular ion peaks [M-H+] of 2554, 2319 and 2377 for HIle, HAla and HAib respectively, in agreement with the expected values.

CD

CD spectroscopy is a particular by useful tool for revealing any structural change that occurs when a complex is formed between two or more macromolecules. In favourable cases, the relative amount of observed change can be related to the quantity of complex formed, so that the K_d and the stoichiometry of complex formation can be estimated.

Since the designed peptides are required to be in helical conformation to interact, all CD experiments were performed in 20% TFE aqueous buffer [38]. Moreover, the buffer/TFE mixture used avoids the bias of non-specific aggregation of the peptides in aqueous buffer.

The CD spectra show spectroscopic features corresponding to an α-helical arrangement (negative maxima at 222 and 205 nm, positive maximum at about 190 nm) [39] (Figure 4). The deconvolution of these spectra *via* a neural network approach [40] gave the secondary structure content values reported in Table 1. Note that the obtained helical percentages, which showed a higher probability of helical conformation for the HAla peptide, are in agreement with the helical propensities predicted by the AGADIR software [41–43].

After measurements on the isolated peptides, titration experiments were carried out to demonstrate the interaction between HIle and HAla and to obtain the stoichiometry and the apparent dissociation constants for complex formation. The HIle/HAla complex was studied by titrating HIle with HAla (Figure 4). In the range of the tested HIle/HAla concentration ratios the 208 nm band of the complex spectra is always deeper than the corresponding band of the theoretical spectra obtained by summing up the spectrum of each isolated peptide. These results indicate that the interaction between the two peptides in the complex induces a conformational change improving the helical folding of one or both peptides. From a thermodynamic point of view this finding suggests an increase in the entropic cost of the complex formation and thus an increase of the corresponding K_d values.

To analyse quantitatively the formation of the complex, the CD results are reported as the difference ($\Delta\theta$) between the $[\theta]_{208}$ ellipticity value of the sum of the spectra of the two peptides and the $[\theta]_{208}$ ellipticity value of the spectrum of the corresponding complex. The $\Delta\theta$ percentage value for the 1 : 1 HIle/HAla ratio, 31.0%, indicates that an interaction between the peptides does take place.

When a 1 : 1 mixture of HAla with the unrelated 20-residue peptide HAib (Ac-^{1}DLRSUKEFUIRS-LRASAMK^{20}-NH_2, where U is the Aib residue) was prepared, the $\Delta\theta$ value of the mixture indicated no interactions (the $\Delta\theta$ percentage values for the 1 : 1 HAla/HAib complex is 0.39%).

The difference spectra between the complex and a linear combination of the free peptides are reported in Figure 4. The spectrum (a) corresponds to the difference obtained for the HAla/HIle complex,

Copyright © 2003 European Peptide Society and John Wiley & Sons, Ltd.

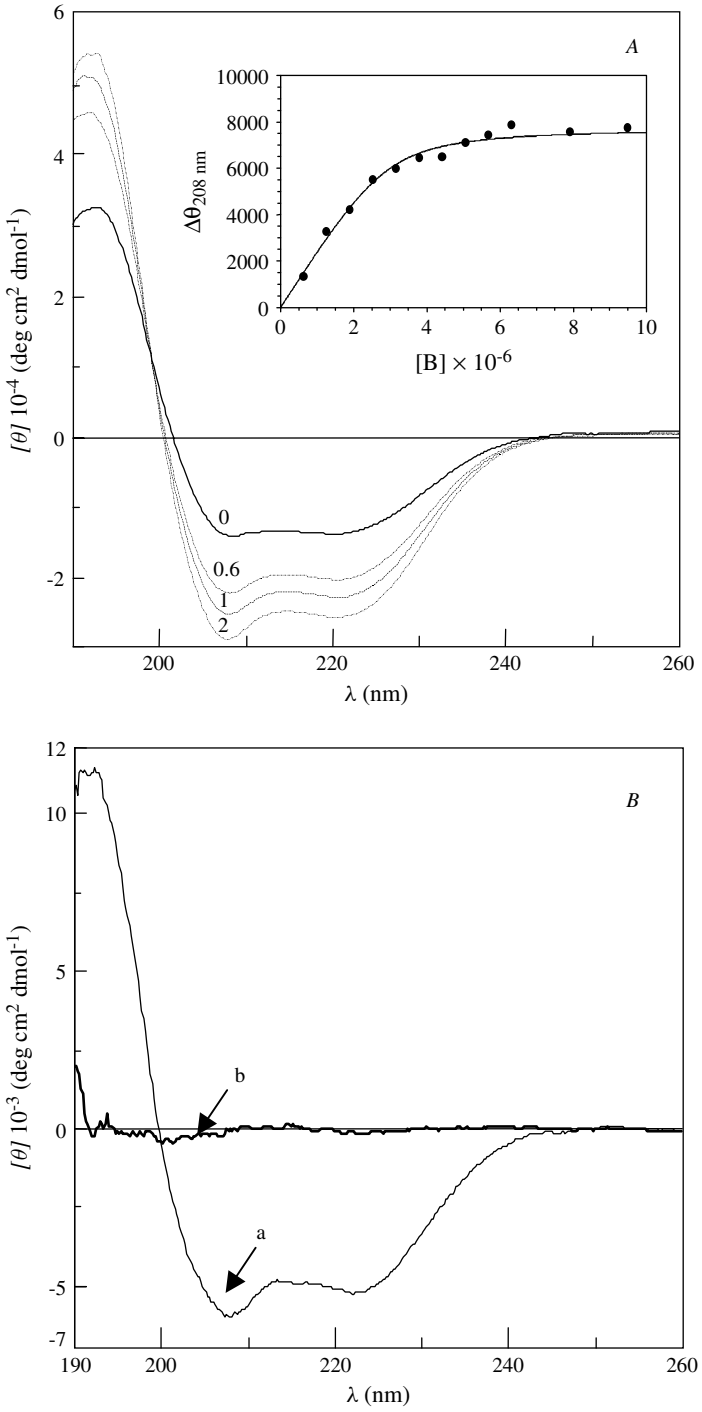

Figure 4 A CD spectra recorded between 190–260 nm at 0, 0.6, 1 and 2 HAla/HIle ratios. The spectra were obtained in 5 mM sodium phosphate buffer at pH 6.7 with 20% TFE. Inset: binding isotherm of the HIle/HAla titration where $[B]_{tot}$ is the total concentration of the peptide to be titrated and $\Delta\theta_{208}$ is the difference between the $[\theta]_{208}$ ellipticity value of the sum of the spectra of the two peptides and $[\theta]_{208}$ ellipticity value of the spectrum of the corresponding complex. B The difference spectra between the complex and a linear combination of the free peptides spectra are reported. The spectrum (a) corresponds to the difference obtained for the HAla/HIle complex, while the spectrum (b) corresponds to the difference obtained for the HAla/HAib complex.

Copyright © 2003 European Peptide Society and John Wiley & Sons, Ltd.

Table 1 Deconvolution Results of the HAla and HIle CD Spectra Obtained Using a Neural Network Approach[40]. All Predicted 'beta Structure' Percentages Were Considered as Extended Conformation

Peptide	Helix (%)	Random coil (%)	Extended conformation (%)	Turns (%)
HIle	44.5	28.4	11.7	15.4
HAla	64.4	17.4	6.5	11.7

while the spectrum (b) corresponds to the difference obtained for the HAla/HAib complex. The obtained difference spectra underline the helical content increase during the HAla/HIle interaction and the absence of effects during the HAla/HAib titration. In order to estimate the apparent dissociation constant of the complex the $\Delta\theta$ value versus total added HAla peptide concentration are reported (Figure 4).

The reported values were fitted by the following binding isotherm [44]:

$$\Delta\theta = [\theta]_c - [\theta]_s = \Delta\theta_{max} \times \frac{([A]_{tot} + [B]_{tot} + K_d) - \sqrt{(K_d + [B]_{tot} + [A]_{tot})^2 - 4[B]_{tot}[A]_{tot}}}{2[B]_{tot}}$$

where $[A]_{tot}$ is the total concentration of HAla added peptide; $[B]_{tot}$ is the total concentration of the peptide to be titrated; K_d is the dissociation constant of complex; $[\theta]_c$ and $[\theta]_s$ are the mean molar ellipticities per residue at 208 nm of the complex and the peptide sum spectra.

To obtain the binding stoichiometry of the HAla/HIle complex, the $[B]_{tot}$ value in the binding isotherm was treated as a variable. The ratio between the fitted value and the total concentration of HAla was found to be 0.93. This result is in agreement with a 1 : 1 binding stoichiometry.

The K_d value for the HAla/HIle is 0.215 μM. This value indicates a binding activity 10^4 smaller than that of IL6 to gp130 (10^{-11} M) and is comparable to the reported binding affinity of some IL6 peptide segments to the receptor-binding region [16]. As outlined above, the observed K_d is increased by the entropy loss due to helix induction in one or both peptides upon complex formation. For this reason a second generation of peptides able to assume a higher helical content should lead to complexes with a stronger binding constant.

NMR HIle Structure

By a careful inspection of TOCSY, NOESY and DQF-COSY spectra almost all the HIle proton resonances were assigned (see Supplementary Materials), following standard procedures [45].

The proton chemical shifts were analysed as described [46], obtaining a peptide helix content of about 53%. The slight helix increase observed by NMR in TFE (30%, v/v) is in reasonable agreement with the above described CD-derived results obtained in TFE (20%, v/v). The lower TFE percentage used for the CD experiments was selected to enhance the detectable variations during the titration.

249 NOE cross peaks were assigned and integrated. Stereospecific assignments for Gln^3 (βCH_2 and γCH_2) and Glu^8 (βCH_2) were derived from the input data using the software DYANA. The NOESY assignments of the HIle peptide showed an extensive H_N–H_N $(i, i+1)$, H_α–$H_N(i, i+3)$ net of cross peaks along the sequence of the peptide (Figure 5), which clearly indicated the presence of a helical structure. Moreover, the lower number of NOESY derived distance constraints for the *N*-terminal portion of the peptide suggested a major flexibility of this region. 20 $^3J_{HNH\alpha}$ coupling constants were extracted from the DQF-COSY spectrum (see Supplementary Material). Since a recent study demonstrated that for peptides dissolved in H_2O/TFE mixtures the amide proton chemical shift changes with increasing temperature may be interpreted by a disruption of intermolecular H-bonds between peptide carbonyl groups and TFE rather than by the disruption of intramolecular H-bonds in α-helices [47], the temperature coefficients of the amide protons of HIle were not measured.

The final input file for the DYANA structure calculation software contained 159 meaningful distance constraints (67 intraresidue, 41 short- and 51 medium-range) and 64 angle constraints which were derived from intraresidue and sequential NOEs and the $^3J_{HNH\alpha}$ coupling constants. These constraints were then used to generate a total of 200 structures and among them the 20 structures with the lowest target function values were selected and energy minimized using the steepest descent algorithm

Copyright © 2003 European Peptide Society and John Wiley & Sons, Ltd.

Figure 5 Diagram of the most representative NOE cross peaks as derived from the NOESY spectrum of the HIle peptide in 5 mM sodium phosphate buffer with 30% TFE, d_3 (v/v).

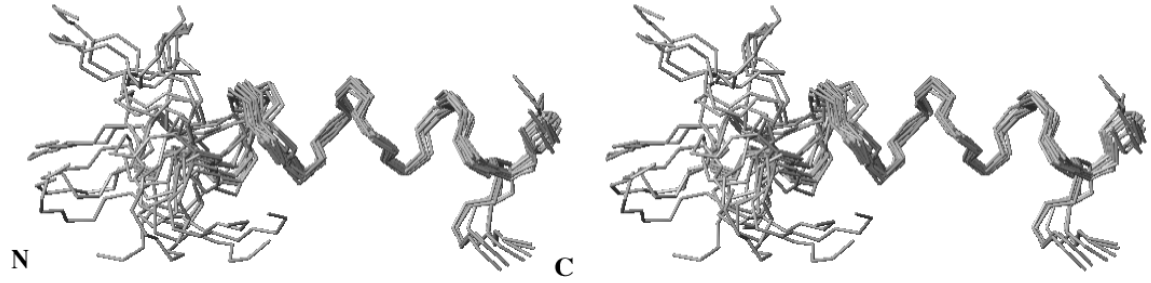

Figure 6 Stereo view of the 20 best HIle DYANA conformers after backbone superposition of the 8–18 residues.

(GROMOS96 force field). The backbone superposition of the best 20 DYANA conformers is reported in Figure 6. In Table 2 the structural statistics for the 20 energy minimized HIle structures are listed.

As evident from Figure 6 the structure of HIle mainly consists of an α helix, whose core is the region 8–18, with a less ordered *N*-terminal part.

A cluster analysis of the HIle structures was performed with the software MOLMOL considering residues 8–20. This analysis underlines that residues 19 and 20 for the most part (65%) are also in a helical conformation. The other accessible conformation is mainly dictated by an alternative (left-handed) conformation of residue 18 ($\varphi = 50^\circ$, $\psi = 60^\circ$) which causes a bend. These results point to a high helical propensity for the usually disordered, *C*-terminal two residues, which show a strong preference for an ordered, helical conformation under the conditions examined.

A representative HIle structure superimposed to the IL6 helix C is reported in Figure 7. It is evident that differences between the two structures is mostly confined to the 1–8 region of HIle, which is mainly an unordered coil. In this region there are the only two residues differing between HIle and helix C of IL6: Lys(Z), which replaces Val^{97} of IL6, and Glu^{8}, which replaces Gln^{98} of IL6.

It could be argued that these two amino acid substitutions have had a 'helix breaker' effect, thereby disorganizing the *N*-terminal part of the helix and differentiating the obtained structure from the designed model. However, the analysis of the two substitutions and a deeper insight into the structure of IL6 show that this is actually not the case.

In the IL6 x-ray diffraction structure the Val^{97} side chain is crucial for packing helix C against the remaining protein, being buried in a pocket constituted by Leu^{21}, Ile^{18}, Gly^{17}, Thr^{14} and Leu^{80}. When the helix is isolated in solution, this pocket is no longer present, so that the corresponding stabilizing interactions are lost, irrespective of the nature of the residue in position 7 of the helix. For this reason this substitution is not specifically related to the observed *N*-terminal helix destabilization.

In the IL6 molecule the $N^{\varepsilon 2}$ atom of Gln^{98} is hydrogen bonded to the $O^{\varepsilon 1}$ atom of Glu^{77}. As in

Copyright © 2003 European Peptide Society and John Wiley & Sons, Ltd.

Table 2 Summary of Conformational Constraints and Statistics for the 20 Structures of the HIle Peptide from NMR Experiments in 30% TFE Phosphate Buffer (v/v)

Meaningful distance constraints	
Intraresidue (i − j = 0)	67
Sequential (|i − j| = 1)	41
Medium-range (2 ≤ |i − j| ≤ 5)	51
Long-range (|i − j| > 5)	0
Total	159
Dihedral angle constraints	
Total	64
$^3J_{HNH\alpha}$	20
RMSD (Å) to the structure with the lowest DYANA target function	
Backbone (overall)	2.463
Backbone (residues 8–18)	0.452
Heavy atoms (overall)	3.397
Backbone (residues 8–18)	1.136
Ramachandran plot	
% residues in the most favourable and additionally allowed region	91
% residues in the generously allowed region	9
% residues in the disallowed region	0
DYANA target function (Å^2)	
Average	0.3545 ± 0.0008
Range	0.20–0.50
Residual violations	
NOE distance constraint violations, maximum (Å)	0.30
Average number of NOE distance constraint violations > 0.2 Å	1.4
Dihedral angle constraint violations, maximum (°)	5.16
Average number of dihedral angle constraint violations > 5°	0.10

the preceding case, this interaction is lost when the helix is separated from the remaining protein.

For the reasons outlined above it seems that the two amino acid substitutions are not directly responsible for the observed 'helix-breaker' effect. On the contrary, the *N*-terminal helix destabilization is due to the loss of stabilizing interactions between helix C and the remainder of IL6. Nevertheless, this helix destabilization does not seem to preclude the ability of HIle to recognize HAla since the binding residues mostly reside in the *C*-terminal portion of the helix, which is the HIle portion more similar to its natural counterpart (Figure 7). This result is in agreement with the reported ability of HIle to bind specifically HAla, as the CD results clearly indicate.

IL6 helix C is a partially amphiphilic structure, with an extensive hydrophobic surface and a smaller hydrophilic surface. Moreover, helix C is not uniformly charged along its axis: the *N*-terminal region is highly charged, while the *C*-terminal region is more hydrophobic. The major occurrence of hydrophobic side chains at the *C*-terminus, and the consequent reduction of amphiphilicity in that region reflect the presumed mechanism of interaction of helix C with gp130, a process mediated by some solvent-exposed hydrophobic residues which interrupt the hydrophilic surface [17].

This finely tuned charge distribution in IL6 helix C is mostly preserved in residues 9–20 of HIle and lost at its *N*-terminus (residues 1–8). In particular, the HIle region 10–18 is nearly identical for charge distribution to the corresponding region of IL6 helix C, due to the good similarity of the side chain three-dimensional arrangement. For the heavy atoms of this region, the average RMSD of helix C, when superimposed to the HIle structure, is 0.976 Å.

The loss of charge distribution similarity in the *N*-terminal region is mainly a consequence of the great mobility of this region in HIle, which produces an average charge distribution different from that of helix C. From a functional point of view the charge density re-organization in HIle with respect to IL6 helix C is not preclusive for bioactivity since most of the HIle contact surface with the target is confined to the *C*-terminus, where the synthetic peptide nicely reproduces the template properties.

NMR Data on HIle–HAla Interaction

The HIle–HAla interaction was followed by NMR techniques after the addition of a 1.1 equivalent of HAla to a 0.8 mM solution of HIle in H_2O/TFE, d_3 (70 : 30, v/v). Before HAla was added, a new set of NMR experiments was performed on the HIle sample in order to check the peptide behaviour at a lower concentration. The analysis of the TOCSY, NOESY and DQF-COSY spectra indicated that at 0.8 mM concentration the HIle proton chemical shifts remain unchanged so that, even if a substantial intensity reduction of the NOE cross-peaks is observed, the original peptide conformation is retained. Thus,

Copyright © 2003 European Peptide Society and John Wiley & Sons, Ltd.

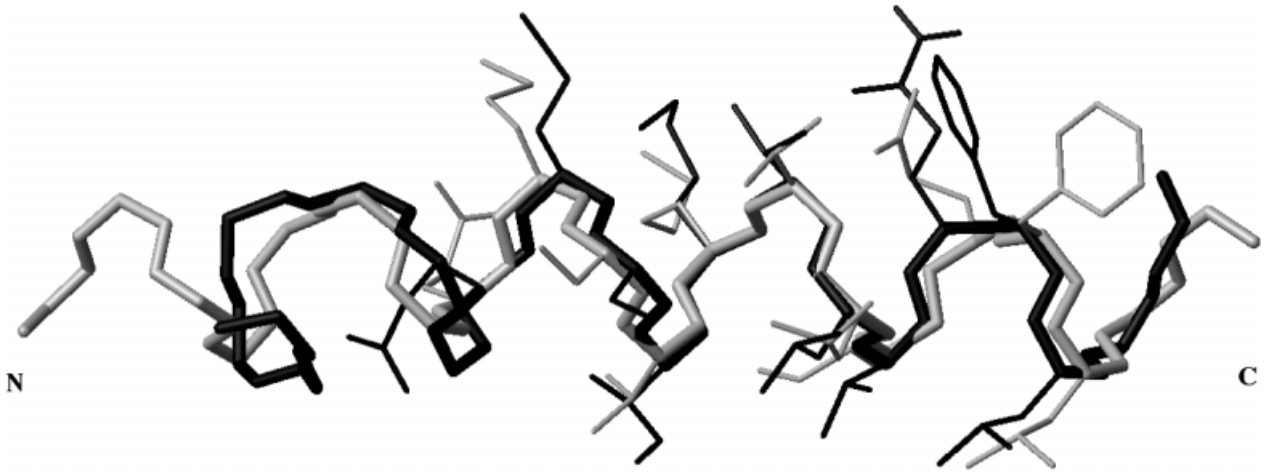

Figure 7 A representative superposition of the backbone and side chains of segment 8–18 of the HIle structure (grey line) with those of the segment 98–108 of helix C (black line) as derived from the IL6 x-ray diffraction structure.

HAla could be added and no precipitation of the complex was observed.

The analysis of the TOCSY and NOESY spectra of the 0.8 mM peptide complex permitted us to fully reassign the HIle proton resonances. Unfortunately, in this case a structure calculation of HIle could not be performed due to the low intensity of the NOE cross-peaks.

The proton chemical shifts of HIle in the complex were analysed as described above, giving a helix content of about 60%. Even if small, the observed HIle helicity increase (7%) is nevertheless equivalent to a helix lengthening of about two residues. In accord with the CD results, these NMR derived data indicate that upon formation of the complex, even in the strongly structuring TFE-rich (30%, v/v) solution, there is a further increase of the peptide helix content. This observation suggests that the helical conformation is required for the interaction and also indicates a possible route to improve the binding efficiency in a second-generation set of peptides.

The backbone sequence-specific assignment of HAla protons turned out to be very difficult because of a strong proton resonance overlapping. This result is mainly a consequence of the high symmetry of the peptide sequence and of its low complexity. Nevertheless, the unambiguous resonance assignment of some non-overlapping residues (Phe^4, Thr^8) of the complex was possible because of their uniqueness in the HAla sequence. Moreover, the ambiguity in the assignment of the two Val residues could be solved by considering that they are connected by a $i, i+4$ H_N–H_N NOE cross-peak and one of them is also connected to Thr^8 through a $i, i+3$ H_N–H_N cross-peak. The identified NOE connectivities and the α-proton chemical shift values of the four assigned residues support the CD indication of a helical structure for HAla.

Interestingly, even if a low number of HAla residues could be assigned, two NOE cross-peaks between the two peptides were unambiguously attributed (Figure 8). In particular, two cross-peaks were assigned between the α-proton of Ala^6(HIle) and the H_N proton of Val^{11}(HAla) and between the βCH_2 protons of Lys^{12}(HIle) and the δ-protons of Phe^4(HAla), respectively. The first relevant information extracted from these data is that the two peptides interact in an antiparallel fashion, as predicted by the modelling and in agreement with the vast majority of known structures of interacting helices.

A second important point is the spacing between the interacting residues in each peptide. The separation between the interacting residues in the two helices ($i, i+6$ in HIle, $i, i+7$ in HAla) is such that each couple of residues is approximately on the same side of the corresponding helix, in agreement with the proposed helix-to-helix interaction.

Tentative Model HIle–HAla Complex

The combined use of all structural parameters derived from the CD and NMR data allowed us to build a tentative model of the solution structure of the HIle/HAla complex.

The two-helix bundle was built using the geometrical parameters of α-helical structures and the two

Copyright © 2003 European Peptide Society and John Wiley & Sons, Ltd.

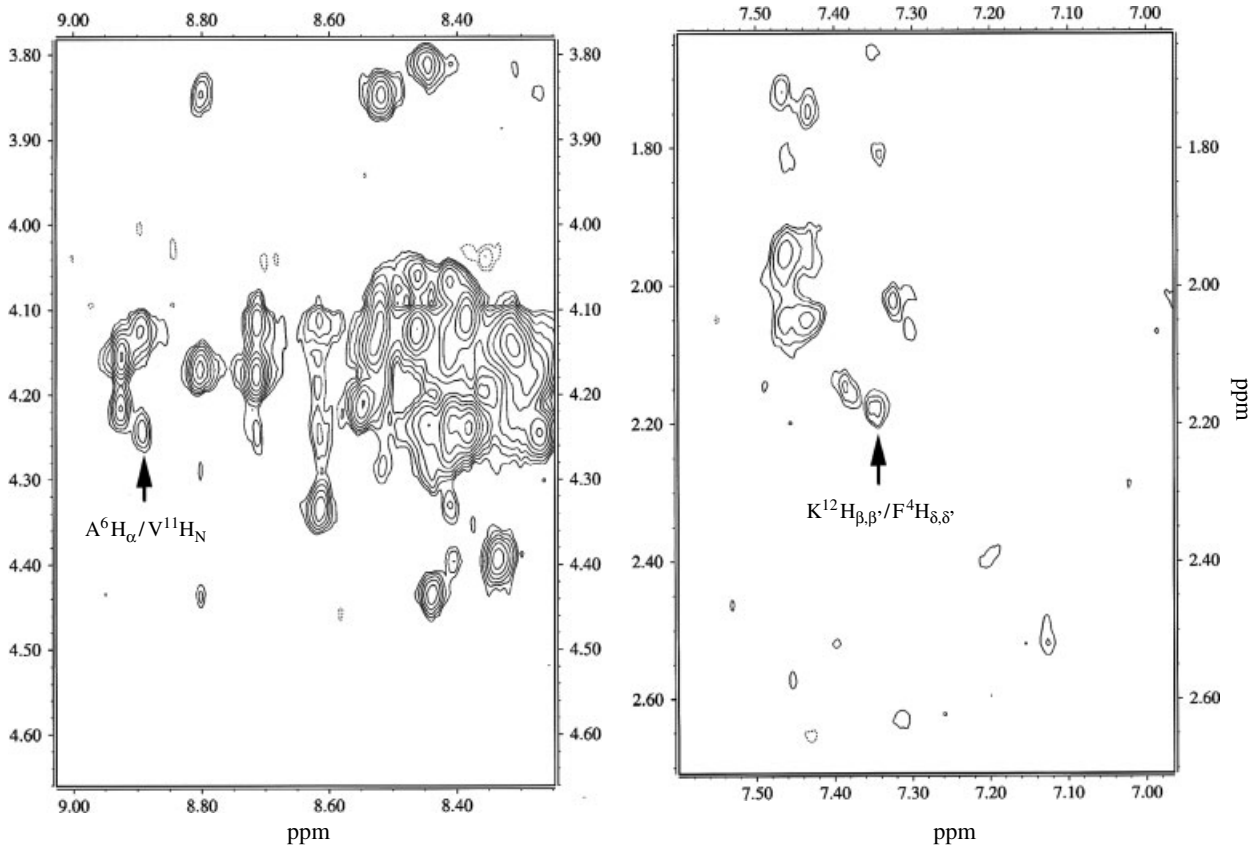

Figure 8 Two regions of the HIle/HAla NOESY spectrum containing two intermolecular NOE cross peaks. The HIle residues are reported as bold characters.

identified intermolecular NOE cross peaks. A qualitative analysis of the intensities of these two NOEs allowed us to classify the Ala^{6}(HIle)···Val^{11}(HAla) and the Lys^{12}(HIle)···Phe^{4}(HAla) contacts as medium and weak, respectively. On these base, the first distance was allowed to vary in the range 3.0–4.0 Å, and the second in the range 4.0–5.0 Å. The dihedral angles of the side chains were modelled by choosing favourable rotamers. A preliminary energy minimization was then carried out by keeping all the backbone atoms fixed to refine the spatial position of the side chains. After this initial step, a full minimization was performed using NMR restraints.

A stereo view of the minimized model is shown in Figure 9. In particular, the two α-helices are antiparallel with an angle of about 25°–30° between their axes. The HIle structure shows a bend in the *N*-terminal part, near the Lys(Z)^{7} residue.

The two-helix bundle structure is stabilized by intermolecular H-bond interactions between the Asp^{1} O$^{\gamma}$ atom of HAla and the Lys^{20} N$^{\varepsilon}$ atom of HIle, between the Asp^{1} O$^{\gamma}$ atom of HAla and the Glu^{16} N$^{\varepsilon}$ atom of HIle, between the Ser^{18} O$^{\gamma}$ atom of HAla and the Glu^{1} O$^{\delta}$ atom of HIle. In addition, some hydrophobic interactions seem to further stabilize the structure.

The analysis of the three-dimensional model of the HIle/HAla complex shows also that some features of the interaction mechanism inferred by NMR differ from those predicted by the modelling. The major differences reside in the HIle interaction side. In particular, an approximately 20° rotation of the HIle interaction surface in the tentative model of the complex was found with respect to that predicted in the theoretical model. This arrangement gives rise to the loss of some predicted interactions between the peptides, e.g. the interaction between HIle Phe^{17} and HAla Phe^{4}.

Other features of the predicted model structure are confirmed by the NMR and CD data. A major point is that, as outlined above, the two peptides must be in a helical conformation to interact. Moreover, the helical arrangement is antiparallel,

Copyright © 2003 European Peptide Society and John Wiley & Sons, Ltd.

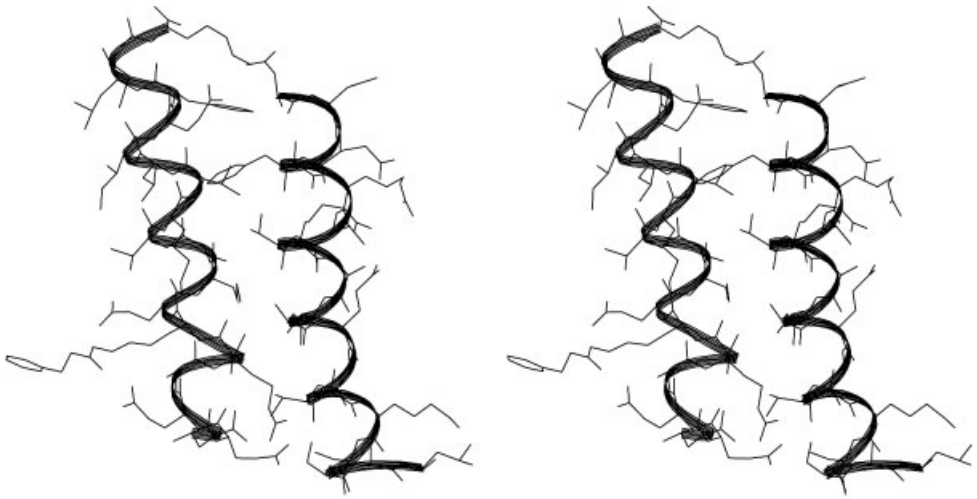

Figure 9 Stereo view of the minimized model of the two-helix bundle structure (HIle/HAla) as obtained by NMR data.

and finally the inferred HAla interaction surface is in good agreement with the modelling prediction.

CONCLUSION

A peptide system was studied by reproducing some of the IL6/gp130 interactions into a two-helix bundle structure. The design of the HAla peptide was performed by selecting the amino acid residues involved in the interaction with the IL6 helix C and using an α-helix scaffold to fit these residues. The titration experiments carried out by use of CD demonstrate that the interaction between HIle and HAla is specific with a well-defined stoichiometry and an apparent dissociation constant of 0.215 μM. In addition, the CD analysis of the peptides confirms their tendency to assume a helical structure. The titration results indicate that upon formation of the complex, even in the strongly structuring TFE solution, there is a further increase of the peptide helix content. This evidence highlights that the α-helix arrangement is required for the HIle/HAla specific interactions.

The study of these peptides and their complex was also carried out by NMR and computational procedures, which allowed us to obtain structural details of the two-helix bundle complexes and to confirm the structural assumptions made in the design process. The NMR data showed differences in some details of the HIle structure and in its complex with HAla, but confirmed the main structural features of the binding mechanism as predicted by the rational design *via* formation of the two-helix bundle. In particular, the most relevant design predictions which are confirmed by NMR data are: (i) the two peptides must be helical to interact; (ii) the HAla surface inferred by NMR to interact with HIle is in agreement with the side predicted to interact by the modelling; (iii) the NMR inferred interhelical angle is very near to that predicted.

These findings are of great interest. Indeed, from a theoretical point of view, they represent an advance in our knowledge of the helix–helix interaction mechanism and indicate a way to target the bioactive helices of proteins *via* the formation of a two-helix bundle. In addition, we have demonstrated that it is possible to characterize in solution two-helix bundle systems, designed without the use of a rigid template or other linkers to connect the helical *N*- and *C*-termini. Obviously, to assess the validity of this approach in the design of new bioactive compounds, more information is needed on the ability of the two peptides to interact with their natural counterparts under more physiological conditions. However, the data reported here represent a promising indication on how to develop fully the described design strategy. From a practical point of view, our data suggest possible improvements to obtain new peptides able to interfere with IL6/gp130 complex formation in an even more effective way. In particular, the reorganization and the helix content increase observed after formation of the complex indicate that the design of a second-generation peptide set should focus on the improvement of

Copyright © 2003 European Peptide Society and John Wiley & Sons, Ltd.

the helicity content of the peptides in aqueous buffer.

Acknowledgements

The authors gratefully acknowledge MURST, the Ministry of University and Scientific and Technological Research (PRIN 2000), and the National Research Council (CNR) of Italy for their continuous and generous support to this research. This work was also supported by Regione Campania Legge 41/94 and by Programma Biotecnologie Legge 95/95 (MURST 5%).

REFERENCES

1. Van Snick J. Interleukin-6: an overview. *Annu. Rev. Immunol.* 1990; **8**: 253–279.
2. Heinrich PC, Castell J, Andus T. Interleukin-6 and the acute phase response. *Biochem. J.* 1990; **265**: 621–636.
3. Akira J, Taga T, Kishimoto T. Interleukin-6 in biology and medicine. *Adv. Immunol.* 1993; **54**: 1–78.
4. Hirano T, Akira S, Taga T, Kishimoto T. Biological and clinical aspects of interleukin 6. *Immunol. Today* 1990; **11**: 443–449.
5. Jilka RL, Hangoc G, Girasole G, Passeri G, Williams DC, Abrams JS, Boyce B, Bromeyer H, Manolagas SC. Increased osteoclast development after estrogen loss: mediation by interleukin-6. *Science* 1992; **257**: 88–91.
6. Poli V, Balena R, Fattori E, Markatos A, Yamamoto M, Tanaka H, Ciliberto G, Rodan GA, Costantini F. Interleukin-6 deficient mice are protected from bone loss caused by estrogen depletion. *EMBO J.* 1994; **13**: 1189–1196.
7. Yamasaki K, Taga T, Hirata Y, Yawata H, Kawanishi Y, Seed B, Taniguchi T, Hirano T, Kishimoto T. Cloning and expression of the human interleukin-6 (BSF-2/IFN beta 2) receptor. *Science* 1988; **241**: 825–828.
8. Hibi M, Murakami M, Saito M, Hirano T, Taga T, Kishimoto T. Molecular cloning and expression of an IL-6 signal transducer, gp130. *Cell* 1990; **63**: 1149–1157.
9. Murakami M, Hibi M, Nakagawa N, Nakagawa T, Yasukawa K, Yamanishi K, Taga T, Tadamitsu K. IL-6-induced homodimerization of gp130 and associated activation of a tyrosine kinase. *Science* 1993; **260**: 1808–1810.
10. Somers W, Stahl M, Seehra JS. 1.9 Å crystal structure of interleukin 6: implications for a novel mode of receptor dimerization and signaling. *EMBO J.* 1997; **16**: 989–997.
11. Bravo J, Staunton D, Heath JK, Jones EY. Crystal structure of a cytokine-binding region of gp130. *EMBO J.* 1998; **6**: 1665–1674.
12. Savino R, Lahm A, Salvati AL, Ciapponi L, Sporeno E, Altamura S, Paonessa G, Tionatti C, Ciliberto G. Generation of interleukin-6 receptor antagonists by molecular-modeling guided mutagenesis of residues important for gp130 activation. *EMBO J.* 1994; **13**: 1357–1367.
13. Savino R, Ciapponi L, Lahm A, Demartis A, Cabibbo A, Toniatti C, Delmastro P, Altamura S, Ciliberto G. The molecular design of human IL-6 receptor antagonists. *EMBO J.* 1994; **13**: 5863–5870.
14. Ciapponi L, Graziani R, Paonessa G, Lahm A, Ciliberto G, Savino R. Definition of a composite binding site for gp130 in human interleukin-6. *J. Biol. Chem.* 1995; **270**: 31 249–31 254.
15. Van Dam M, Müllberg MJ, Schoolting H, Stoyan T, Brakenhoff JPJ, Greave L, Henrich PC, Rose-John S. Structure-function analysis of interleukin-6 utilizing human/murine chimeric molecules. Involvement of two separate domains in receptor binding. *J. Biol. Chem.* 1993; **268**: 15 285–15 294.
16. Ekida T, Nishimura C, Masuda S, Itoch S, Shimada I, Arata Y. A receptor-binding peptide from human interleukin-6: isolation and a proton nuclear magnetic resonance study. *Biochem. Biophys. Res. Commun.* 1992; **189**: 211–220.
17. Menziani MC, Fanelli F, De Benedetti PG. Theoretical investigation of IL-6 multiprotein receptor assembly. *Proteins* 1997; **29**: 528–544.
18. Lifson S, Hagler AT, Dauber PJ. Consistent force field studies of intermolecular forces in hydrogen-bonded crystals. 1. Carboxylic acids, amides, and the C=O···H hydrogen bonds. *J. Am. Chem. Soc.* 1979; **101**: 5111–5121.
19. Hagler AT, Lifson S, Dauber PJ. Consistent force field studies of intermolecular forces in hydrogen-bonded crystals. 2. A benchmark for the objective comparison of alternative force fields. *J. Am. Chem. Soc.* 1979; **101**: 5122–5130.
20. Hagler AT, Dauber PJ, Lifson S. Consistent force field studies of intermolecular forces in hydrogen-bonded crystals. 3. The C=O···H–O hydrogen bond and the analysis of the energetics and packing of carboxylic acids. *J. Am. Chem. Soc.* 1979; **101**: 5131–5140.
21. Marion D, Ikura M, Tschudin R, Bax A. Rapid recording of 2D NMR spectra without phase cycling: application to the study of hydrogen exchange in proteins. *J. Magn. Reson.* 1989; **85**: 393–399.
22. Bax A, Davis DG. MLEV-17-based two-dimensional homonuclear magnetization transfer spectroscopy. *J. Magn. Reson.* 1985; **65**: 355–360.
23. Jeener J, Meier BH, Bachmann P, Ernst RR. Investigation of exchange processes by two-dimensional NMR spectroscopy. *J. Chem. Phys.* 1979; **71**: 4546–4553.
24. Rance M, Sorensen OW, Bodenhausen G, Wagner G, Ernst RR, Wüthrich K. Improved spectral resolution in

Copyright © 2003 European Peptide Society and John Wiley & Sons, Ltd.

COSY ^{1}H NMR spectra of proteins via double quantum filtering. *Biochem. Biophys. Res. Commun.* 1983; **117**: 479–485.
25. Güntert P, Dötsch V, Wider G, Wüthrich K. Processing of multi-dimensional NMR data with the new software PROSA. *J. Biomol. NMR* 1992; **2**: 619–629.
26. Bartels C, Xia T, Billeter M, Güntert P, Wüthrich K. The program XEASY for computer-supported NMR spectral analysis of biological macromolecules. *J. Biomol. NMR* 1995; **6**: 1–10.
27. Güntert P, Mumenthaler C, Wüthrich K. Torsion angle dynamics for NMR structure calculation with the new program DYANA. *J. Mol. Biol.* 1997; **273**: 283–298.
28. Van Gusteren WF, Billeter SR, Eising AA, Hunenberger PH, Kruger P, Mark AE, Scott WRP, Tironi IG. *Biomolecular Simulation: The GROMOS96 Manual and User Guide*. BIOMOs: Zürich, Switzerland.
29. Koradi R, Billeter M, Wüthrich K. MOLMOL: a program for display and analysis of macromolecular structures. *J. Mol. Graph.* 1996; **14**: 51–55.
30. Karle LI, Flippen-Anderson JL, Uma K, Balaram P. Helix aggregation in peptide crystals: occurrence of either all parallel or antiparallel packing motifs for α-helices in polymorphs of Boc-Aib-Ala-Leu-Ala-Leu-Aib-Leu-Ala-Leu-Aib-OMe. *Biopolymers* 1990; **29**: 1835–1845.
31. Marqusee S, Baldwin RL. Helix stabilization by $Glu^- \ldots Lys^+$ salt bridges in short peptides of *de novo* design. *Proc. Natl Acad. Sci. USA* 1987; **84**: 8898–8902.
32. Brooks BR, Bruccolieri RE, Olafson BD, States DJ, Swaminathan S, Karplus M. CHARMM: a program for macromolecular energy, minimization, and dynamics calculations. *J. Comput. Chem.* 1983; **4**: 187–217.
33. Chou CK, Zhang CT, Maggiora GM. Disposition of amphiphilic helices in heteropolar environments. *Proteins* 1997; **28**: 99–108.
34. Forood B, Feliciano EJ, Nambiar KP. Stabilization of α-helical structures in short peptides via end capping. *Proc. Natl Acad. Sci. USA* 1993; **90**: 838–842.
35. Pavone V, Gaeta G, Lombardi A, Nastri F, Maglio O, Isernia C, Saviano M. Discovering protein secondary structures: classification and description of the α-turn. *Biopolymers* 1996; **38**: 705–721.
36. Coste J, Le-Nguyen D, Castro B. PyBOP: a new peptide coupling reagent devoid of toxic byproducts. *Tetrahedron Lett.* 1990; **31**: 201–208.
37. Carpino LA. 1-Hydroxy-7-azabenzotriazole. An efficient peptide coupling additive. *J. Am. Chem. Soc.* 1993; **115**: 4397–4398.
38. Jasanoff A, Fersht AR. Quantitative determination of helical propensities from trifluoroethanol titration curves. *Biochemistry* 1994; **8**: 2129–2135.
39. Yang JT, Wu CSC, Martinez HM. Calculation of protein conformation from circular dichroism. *Methods Enzymol.* 1986; **130**: 208–269.
40. Bohm G, Muhr R, Jaenicke R. Quantitative analysis of protein far-UV circular dichroism spectra by neural networks. *Protein Eng.* 1992; **5**: 191–195.
41. Münoz V, Serrano L. Elucidating the folding problem of helical peptides using empirical parameters. *Nature Struct. Biol.* 1994; **1**: 399–409.
42. Münoz V, Serrano L. Elucidating the folding problem of helical peptides using empirical parameters. II. Helix macrodipole effects and rational modification of the helical content of natural peptides. *J. Mol. Biol.* 1995; **245**: 275–296.
43. Münoz V, Serrano L. Elucidating the folding problem of helical peptides using empirical parameters. III. Temperature and pH dependence. *J. Mol. Biol.* 1995; **245**: 297–308.
44. Wisz MS, Garrett CZ, Hellinga HW. Construction of a family of Cys2His2 zinc binding sites in the hydrophobic core of thioredoxin by structure-based design. *Biochemistry* 1998; **37**: 8269–8277.
45. Wüthrich K. In *NMR of Proteins and Nucleic Acids*. Wiley: New York, 1986.
46. Lee MS, Cao B. Nuclear magnetic resonance chemical shift: comparison of estimated secondary structures in peptides by nuclear magnetic resonance and circular dichroism. *Protein Eng.* 1996; **9**: 15–25.
47. Rothemund S, Weisshoff H, Beyermann M, Krause E, Bienert M, Mugge C, Sykes BD, Sonnichsen FD. Temperature coefficients of amide proton NMR resonance frequencies in trifluoroethanol: a monitor of intramolecular hydrogen bonds in helical peptides. *J. Biomol. NMR* 1996; **8**: 93–97.

Copyright © 2003 European Peptide Society and John Wiley & Sons, Ltd.